JOURNAL OF MATERIALS SCIENCE **34** (1999) 4425–4437

Cast and aged β-NiAl-β'-Ni_2AlTi-γ'-Ni_3Al-α-Cr alloys: a microstructural and mechanical properties investigation

W. F. GALE, Z. A. M. ABDO
Materials Research and Education Center, Auburn University, 201 Ross Hall, Auburn, AL 36849, USA
E-mail: wfgale@eng.auburn.edu

Microstructural development and stability in cast Ni-30 at % Al-21 at % Cr-4 at % Ti, Ni-28 at % Al-18 at % Cr-6 at % Ti and Ni-26 at % Al-19 at % Cr-8 at % Ti alloys are examined in this paper. The paper considers the extent to which microstructural control and stability is improved in these alloys, when compared with earlier work by the authors on similar materials with lower aluminum (25 or 26 at %) and higher titanium (11 to 15 at %) contents. The paper discusses detailed transmission electron microscopy investigations of both as-cast and aged (140 h at 850 and 1100 °C) samples. Attention is focussed on the transformation of $L2_1$ type β' (nominally Ni_2AlTi) dendrites. In particular, the influence of the formation of intradendritic $L1_2$ type γ' (nominally $Ni_3(Al,Ti)$) on the stability of the β'-phase is examined. Morphological changes and phase transformations within a β'-α-Cr eutectic are discussed. Various modes of second-phase precipitation are considered. The microstructures of selected samples are correlated with mechanical properties determined by tensile testing and fractography.

1. Introduction

The B2 type structural intermetallic compound NiAl (the "β" phase) suffers from a lack of room-temperature ductility/toughness and has only limited high-temperature creep resistance [1]. Ductilisation/ toughening of the β-phase may be achieved by means of the addition of various second phases [2–8], such as γ (face-centered cubic nickel, iron or copper-base solid-solution), γ' ($L1_2$ type intermetallic, nominally $Ni_3(Al,Ti)$ or a γ/γ' two phase mixture. Furthermore, the fracture toughness of NiAl may be enhanced significantly by the formation of NiAl-α eutectic, for which the α-phase represents a body centered cubic solid solution (based on chromium or molybdenum). In contrast, the creep resistance of NiAl is increased substantially [9] by the addition to the β matrix of an $L2_1$ type second phase (Heusler type phase [10, 11], such as Ni_2AlTi or Ni_2AlHf, denoted as β').

In previous work by the authors, an attempt was made to develop microstructures which are capable of benefiting both from: (a) ductilisation/toughening due to the presence of γ' and/or eutectics involving α-Cr and (b) enhanced creep resistance due to the formation of two phase β/β'. This work involved cast nickel-rich Ni-Al-Cr-Ti alloys containing: 25 or 26 at % Al, 20 to 24 at % Cr and 11 to 15 at % Ti. The microstructures developed in these systems were rather complex. This complexity was the result, at least in part, of the combined effects of rejection of chromium by the growing β or β' phase during solidification and the precipitation of both intra- and interdendritic γ'. Nonetheless, this work established the possibility of forming interdendritic β/β' by the partial transformation of the β constituent of a β-α eutectic. However, the dendrite matrices of these alloys were single phase and consisted of either β or β', not both.

In response to the microstructures generated in the Ni-Al-Cr-Ti alloys described above, the present paper examines the extent to which the formation of stable β/β' phase mixture can be enhanced in this system by increasing the ratio of aluminum to titanium, while holding the chromium content approximately constant. Intuitively, partial substitution of aluminum for titanium might be expected to favor the formation of β over β'. However, as will be shown in this paper, this was by no means universally the case.

The present paper considers the microstructural development and stability in cast Ni-30 at % Al-21 at % Cr-4 at % Ti, Ni-28 at % Al-18 at % Cr-6 at % Ti and Ni-26 at % Al-19 at % Cr-8 at % Ti alloys in both the as-cast and aged conditions. Heat treatment temperatures of 850 and 1100 °C and an aging time of 140 h were chosen for this work. This choice of thermal exposures was based on earlier work by one of the authors (on the decomposition of aluminide diffusion coatings [12–14] and bulk microstructural analogues to these coatings [15, 16]). These analogues have microstructures with features common to the class of materials investigated in the present work.

Attention is focussed on the transformation of $L2_1$ type β' (nominally Ni_2AlTi) dendrites to different degrees. In particular, the influence of the formation

of intradendritic $L1_2$ type γ' (nominally $Ni_3(Al,Ti)$) on the stability of the β'-phase is examined. Morphological changes and phase transformations within a β'-α-Cr eutectic are considered. A variety of second-phase precipitation processes are also examined.

Given the difficulty of achieving room-temperature ductility in creep-resistant NiAl-based materials, an investigation of room-temperature tensile properties was undertaken. Based on the microstructural investigations, the Ni-28 at % Al-18 at % Cr-6 at % Ti alloy was taken as being "typical" of the class of intermetallic considered by the authors in the present work (and the earlier paper from which the research described in this paper originated). Hence, the mechanical properties of the Ni-28 at % Al-18 at % Cr-6 at % Ti alloy were investigated in the as-cast condition as well as after aging for 140 h at both 850 and 1100 °C. Correlations are drawn between the microstructure of this material in the different conditions considered and observed mechanical properties.

2. Experimental

Ni-30 at % Al-21 at % Cr-4 at % Ti, Ni-28 at % Al-18 at % Cr-6 at % Ti and Ni-26 at % Al-19 at % Cr-8 at % Ti samples were prepared as 30 g arc-melted buttons. In order to increase the homogeneity of these materials, each button was inverted and remelted six times. Samples of these materials were heat treated at temperatures of 850 and 1100 °C for a duration of 140 h, followed by furnace cooling to room temperature.

The microstructures of as-cast, plus 850 and 1100 °C heat treated samples of all of the materials considered, were examined in detail using transmission electron microscopy (TEM) using a JEOL JEM 2010 instrument, operated at 200 kV. In this paper the following nomenclature is employed: bright field and dark field micrographs are denoted respectively by "BF" and "DF", selected area diffraction patterns with a beam direction of "**B**" are indicated by "SAD" and "**g**" is the reciprocal lattice vector of the reflection used to form DF images. The TEM work was complimented by light microscopy (LM) and scanning electron microscopy (SEM) investigations, the latter performed using a JEOL JSM 840 microscope, operated at 20 kV. Quantitative SEM-based and qualitative TEM-based energy dispersive X-ray spectroscopy was performed using Oxford Instruments Link ISIS analyzers and ultrathin window (UTW) detectors attached to the JEOL 2010 and 840 instruments.

The authors have previously experienced problems with jet polishing TEM specimens from the type of material examined here. In electropolished samples of this type of material, severe differential polishing was observed, associated with the inhomogeneous distribution of aluminum and chromium in the specimens. Hence, in the present work, ion milling was used in preference to electropolishing. TEM specimens were prepared by dual-gun, liquid nitrogen cooled stage argon ion milling in a Gatan DuoMill operated at 5 kV with gun—specimen angles of 13° and gun currents of 500 μA per gun. Where possible, SEM-based EDS analysis was performed on polished, unetched samples. Metallographic samples for light microscopy, SEM-based secondary electron imaging (SEI) and EDS on individual phases were electroetched at 3 V in a solution made up of 30% acetic acid, 30% lactic acid, 20% hydrochloric acid, 10% nitric acid and 10% distilled water.

Tensile testing was performed on samples with a gauge length of 8 mm and an initial cross-sectional area of 5.25 mm^2. These samples were tested at a grip separation rate of 8×10^{-4} mm per min. Prior to tensile testing, all specimens were electropolished in a solution of 25% nitric acid in methanol at a temperature of -20 °C and current density of 3.5 mA mm^{-2} to minimize surface scratches. SEM-based fractography was conducted on the tensile samples.

3. Results and discussion

The compositional and microstructural features of the materials considered in this paper are summarized respectively in Tables I and II, for both the as-cast and (850 and 1100 °C) aged conditions. The nature and origins of the various microstructural features listed in Table II will now be discussed.

3.1. Dendritic β and β' phases

In the as-cast condition (Fig. 1), all of the materials examined solidified dendritically (Fig. 1a) with single-phase β' matrices. At first sight, this seems surprising, given the low titanium content (3–7 at %) listed in Table I for the dendritic regions of the samples. Furthermore, a far higher average dendritic titanium content (11 at %) was associated with the formation of β-phase dendrites in previous work. However, it must be borne in mind that the compositions listed in Table I are averages for each region and include numerous second phase precipitates.

TABLE I Compositions of the dendritic and interdendritic regions of the materials examined (data from SEM-based EDS analyses). Note: phases present on the dendrite boundaries are not included in these data

Overall as-cast composition (at %)				As-cast (at %)								Aged 140 h at 850 °C (at %)								Aged 140 h at 1100 °C (at %)							
				Average dendritic composition				Average interdendritic composition				Average dendritic composition				Average interdendritic composition				Average dendritic composition				Average interdendritic composition			
Ni	Al	Cr	Ti	Ni	Al	Cr	Ti	Ni	Al	Cr	Ti	Ni	Al	Cr	Ti	Ni	Al	Cr	Ti	Ni	Al	Cr	Ti	Ni	Al	Cr	Ti
ba	30	21	4	ba	36	10	3	ba	22	41	3	ba	36	11	3	ba	25	36	3	ba	35	9	1	ba	20	21	4
ba	28	18	6	ba	37	9	4	ba	7	16	17	ba	40	10	4	ba	17	49	4	ba	37	7	7	ba	4	89	1
ba	26	19	8	ba	34	10	7	ba	8	17	16	ba	36	9	16	ba	3	78	4	ba	31	6	8	ba	6	74	4

TABLE II Summary of the microstructural features of the materials examined in the as-cast and aged conditions

Overall as-cast composition (at %)				As-cast (at %)				Aged 140 h at 850 °C (at %)				Aged 140 h at 1100 °C (at %)			
				Dendritic region		Interdendritic region		Dendritic region		Interdendritic region		Dendritic region		Interdendritic region	
Ni	Al	Cr	Ti	Matrix	Second phases	Matrix	Second phases	Matrix	Second phases	Matrix	Second phases	Matrix	Second phases	Matrix	Second phases
ba	30	21	4	β'	α γ' ppt in bulk layer γ' needle layer near dend bndry	β'-α lam eutc	γ' in eutc β'	β	α γ' ppt in bulk dend γ' needle layer near dend bndry	β-α trans lam eutc	γ' in trans eutc β	β	α γ'	β'-α agglom eutc	none
ba	28	18	6	β' β in regns close to γ' clny	γ' ppt and clny α	β'-α lam eutc	γ' clny	β/β' β' PFZ near γ'	γ' ppt and clny	β/β'-α trans lam eutc	γ'	β	α γ'	β-α trans lam eutc	none
ba	26	19	8	β' β in regns close to γ' layer	$L1_0$ mart α γ' clny γ' needle layer near dend bndry	β'-α lam eutc	β in eutc α γ' clny	β'	"$\frac{1}{4}$" needle ppt esp on dend bndry	β'-α lam eutc	β in eutc α	β'	α	β'-α agglom eutc	β in eutc α

Based on qualitative TEM-based EDS, in general, the overall dendritic titanium content was largely contained within the dendrite matrix. Hence, the formation of β' dendrites is less surprising than might be thought. An important exception to this situation occurred in regions containing colonies of γ' precipitates (the formation of γ' is discussed in detail in Section 3.3). Where a large amount of γ' was produced, the formation of γ' had the effect of denuding the dendrite matrix in titanium. In the titanium depleted regions, transformation of the dendrite matrices from β' to β was observed (Fig. 1b). The resulting β-phase regions were extremely large and often extended up to 5–10 μm from the edge of the γ' colonies. In the Ni-26 at % Al-19 at % Cr-8 at % Ti alloy, strongly nickel-rich regions of the dendrites were found to have $L1_0$ type martensitic matrices in the as-cast condition (Fig. 1c). However, the $L1_0$ phase transformed to β' on aging.

Aging of the three alloys did not have a systematic effect on the average composition of the dendrites. Nonetheless, the 850 and 1100 °C heat treatments destabilized the β'-phase in the 4 and 6 at % Ti alloys. In the case of the 6 at % Ti material aged at 850 °C, only partial transformation of the β'-phase was observed, resulting in the formation of two phase β/β' mixture (Fig. 2). However, this was the only condition for which two phase β/β' was produced and this does not augur well for the stability of this desirable microstructure. In the 850 °C aged condition, the 6 at % Ti material contained numerous fine individual γ' precipitates (as is discussed in Section 3.3 below). In common with the γ' colonies, these individual γ' precipitates had the effect of denuding the surrounding matrix of titanium and preventing the formation of β' precipitates. Hence, precipitate free zones (PFZs) were formed around the γ' precipitates. These PFZs were far smaller than the large β-phase regions around γ' colonies (as described above). Typically, the PFZs did not extend further than 100–200 nm from the edge of the γ' precipitates.

3.2. β'-α eutectic

In all of the materials examined (Fig. 3), solidification terminated with the formation of a β'-α lamellar eutectic mixture (Fig. 4) with the β' and α phases cube—cube orientation related. This eutectic mixture was morphologically similar to that observed in the higher titanium materials investigated in previous work [17]. A tendency was noted for the precipitation of fine β (typically around 20–100 nm in diameter) within the α constituent of the β'-α eutectic (Fig. 5).

In general, the stability of the eutectic β' phase during thermal exposure followed that of the dendrite matrices and so both β-α and β/β'-α transformed eutectics were observed in the aged samples. However, a significant divergence in behavior was observed between the dendritic and eutectic β' phases, as will now be discussed.

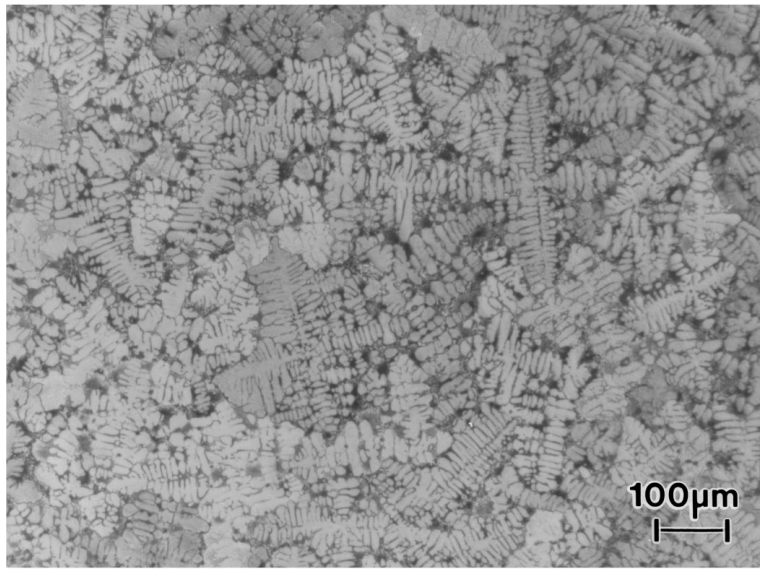

(a)

(b)

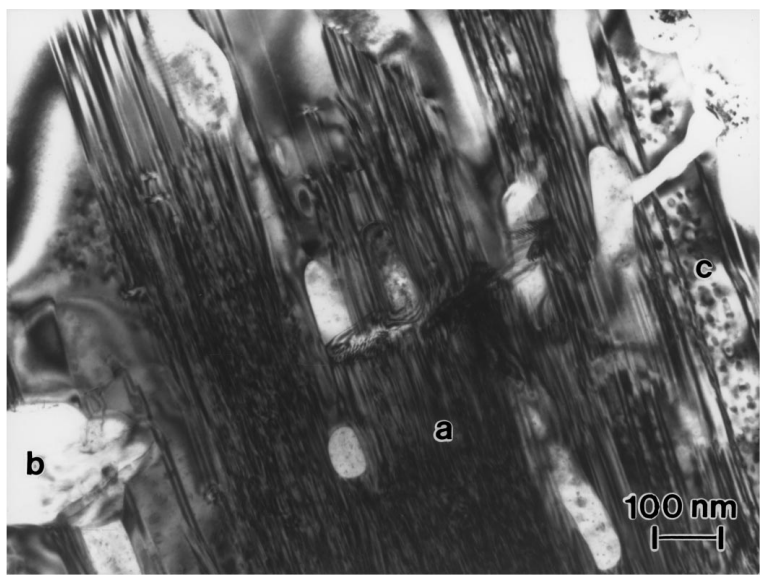

(c)

Figure 1 Dendritic microstructures observed in the as-cast condition: (a) Light micrograph showing β' dendrites and β'-α eutectic in the Ni-30 at% Al-21 at% Cr-4 at% Ti material. (b) Formation of β regions in the vicinity of the γ' phase. SAD pattern with $\mathbf{B} = [1\,1\,0]_{\beta}$. Note the absence of β' type reflections. (c) BF micrograph showing $L1_0$ type martensite (labeled as "a"). Note also the presence of γ' (marked as "b") and α-Cr with β precipitates (regions denoted by "c").

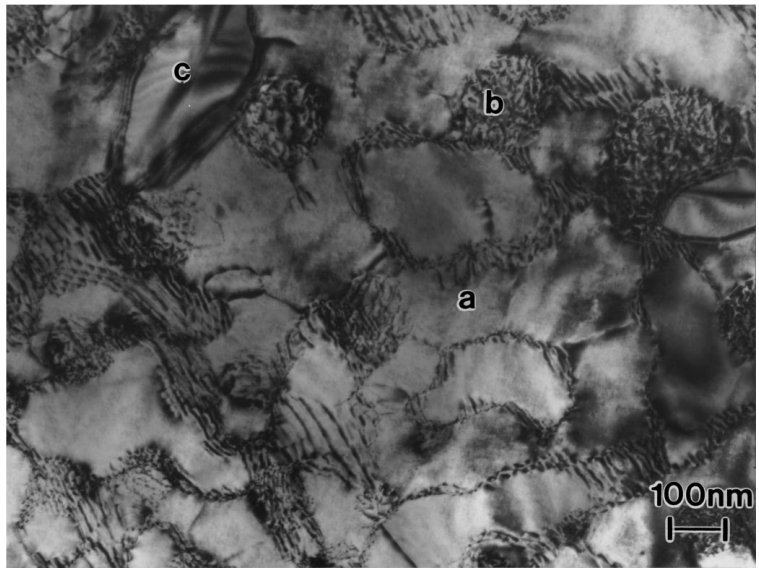

(a)

(b)

Figure 2 Two phase β/β' present in the Ni-28 at % Al-18 at % Cr-6 at % Ti alloy after aging at 850 °C for 140 h: (a) BF micrograph showing two phase β/β' (labeled as "a"), plus α-Cr (marked as "b") and twinned γ' precipitates (denoted by "c"). (b) SAD pattern with $\mathbf{B} = [1\,1\,0]_{\beta/\beta'}$. Compare this pattern with Fig. 1b and note the additional β' reflections.

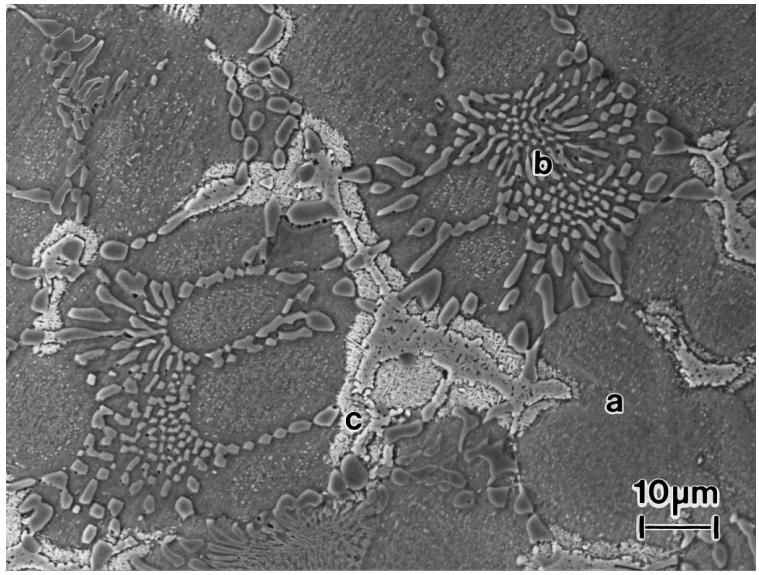

Figure 3 Overall microstructure of the as-cast Ni-26 at % Al-19 at % Cr-8 at % Ti alloy (SEI). Note the presence of β' dendrites (labeled as "a"), β'-α eutectic (marked as "b") and a layer of γ' needles in the vicinity of the dendrite boundaries (regions denoted by "c").

Figure 4 BF micrograph showing the β'-α eutectic present in the as-cast Ni-26 at % Al-19 at % Cr-8 at % Ti alloy. In this image, the α-Cr appears as the lighter toned features and the β' as the darker toned regions.

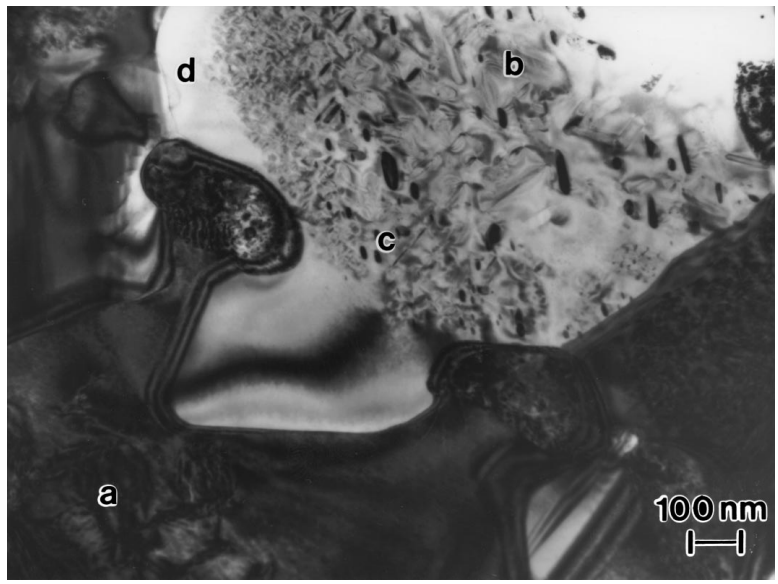

Figure 5 Dendrite boundary region of the as-cast Ni-26 at % Al-19 at % Cr-8 at % Ti material, imaged in BF ("a" is the dendritic area and "b" the interdendritic region). The portion of the interdendritic region shown in this micrograph consists of the α constituent of the β'-α-Cr eutectic. This α-Cr contains numerous β precipitates (labeled as "c"). Note the formation of a precipitate free zone (marked as "d"), corresponding with a portion of the α-Cr, adjacent to the β' dendrite, that was low in nickel and aluminum.

For reasons that are unclear at the present time, γ' that precipitated interdendritically was far lower in titanium than intradendritic γ'. This disparity in the titanium content did not seem to be tied to the overall titanium content of the region in which the γ' precipitated.

Regardless of the origin of the difference in titanium content between the intra- and interdendritic regions, the effects of this situation on the stability of the β' phase were clearly observable. The formation of interdendritic γ' with a low titanium content correlated with the partial transformation of β' to β and hence resulted in a β/β' two phase mixture in the 6 at % titanium alloy after the 850 °C aging treatment. The role of γ' in depleting the β' matrix of titanium was clearly evident in the Ni-28 at % Al-18 at % Cr-6 at % Ti alloy, where the interdendritic titanium content fell from 17 at % in the as-cast condition to 4 at % after 850 °C aging. In this material, the β' was not completely eliminated by the aging treatment.

Destabilization of the interdendritic β' phase in favor of β did not invariably correlate with depletion of titanium from the interdendritic regions. For example, the interdendritic β' from the Ni-30 at % Al-21 at % Cr-4 at % Ti alloy was fully transformed back to β, after aging at 850 °C. However, the overall composition of the interdendritic region remained similar to that in the as-cast condition (see Table I). These results suggest that depletion of titanium was not the sole deciding factor in the stability of the interdendritic β' phase. Indeed, given the complex microstructure of these materials, the processes governing the stability of β' are not entirely clear.

Aging at 1100 °C had a tendency to encourage agglomeration of the eutectic α-phase (although this could

not be described as truly spheroidised). However, unlike the higher (11–15 at %) titanium materials examined in previous work, this agglomeration process was not accompanied by extensive growth of the dendrites at the expense of the interdendritic region. Hence, in the present work, a tendency for the formation of rump interdendritic regions comprised entirely of γ' was not observed.

3.3. Second phase precipitation

The most prominent second phase observed in the alloys examined here was γ'. Three distinct modes of γ' precipitation were observed. However, in all cases a Kurdjumov–Sachs type orientation relationship, such that:

$$(1\,1\,1)_{\gamma'} \parallel (1\,1\,0)_{\beta}$$
$$[0\,\bar{1}\,1]_{\gamma'} \parallel [1\,\bar{1}\,1]_{\beta}$$

was observed (Fig. 6) between the γ' and the β (or β') matrix. The first of the three modes of γ' precipitation was the formation of individual precipitates. These precipitates were observed both intra- and interdendritically, especially after 850 °C aging. In general, these precipitates were midrib twinned (Fig. 7), although non-twinned precipitates were also observed. Midrib twinned γ' is commonly observed in aged materials derived from nickel-rich NiAl [10].

A second type of γ' precipitation observed in the present work was the formation of a layer of γ' needles at the dendrite boundaries (Fig. 3). Such layers were also observed in previous work by the authors on higher (11–15 at %) titanium materials. However, in the present case the γ' layer was orientation related to the dendrites. Whereas, in the higher titanium alloys, the layer formed with an orientation relationship to the interdendritic region (in all cases no orientation

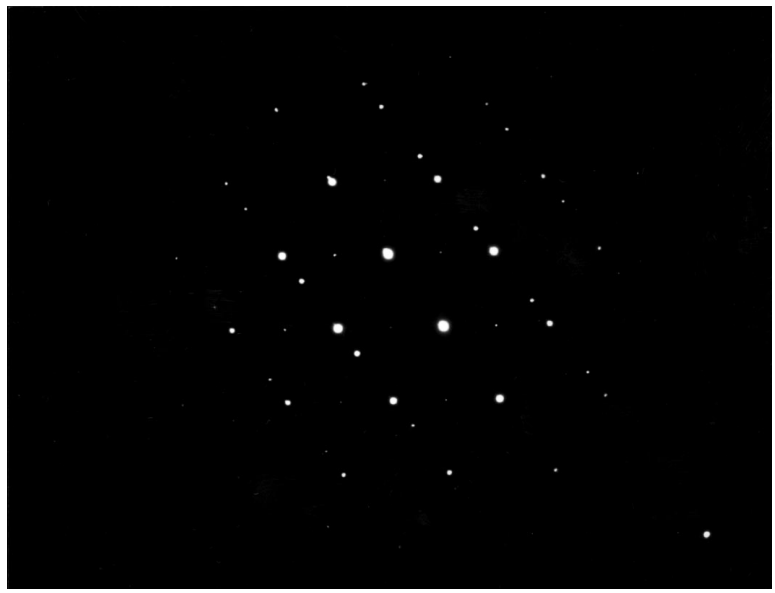

(a)

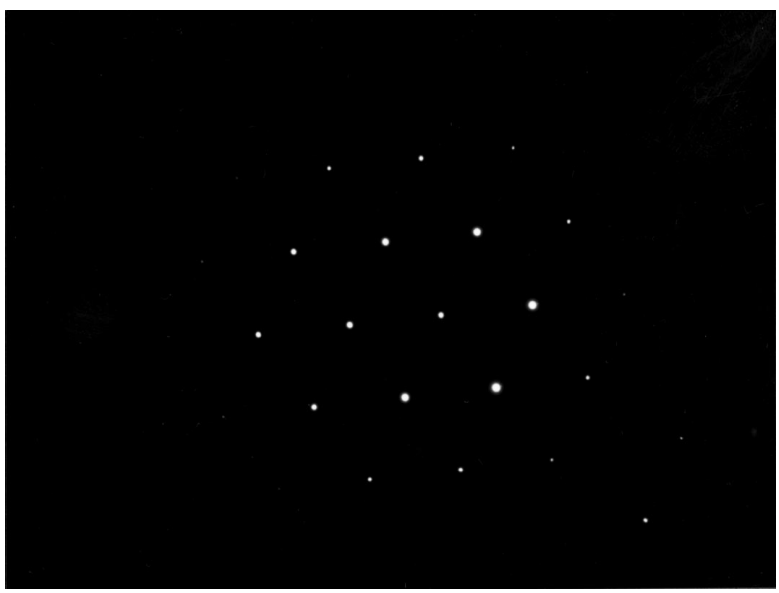

(b)

Figure 6 SAD patterns illustrating the Kurdjumov–Sachs orientation relationship between the β and γ' phases (Ni-30 at % Al-21 at % Cr-4 at % Ti alloyed aged for 140 h at 850 °C): (a) $\mathbf{B} = [0\,\bar{1}\,1]_{\gamma'}$; (b) $\mathbf{B} = [1\,\bar{1}\,1]_{\beta}$; (c) $\mathbf{B} = [0\,\bar{1}\,1]_{\gamma'} \parallel [1\,\bar{1}\,1]_{\beta}$. (*Continued*).

(c)

Figure 6 (*Continued*).

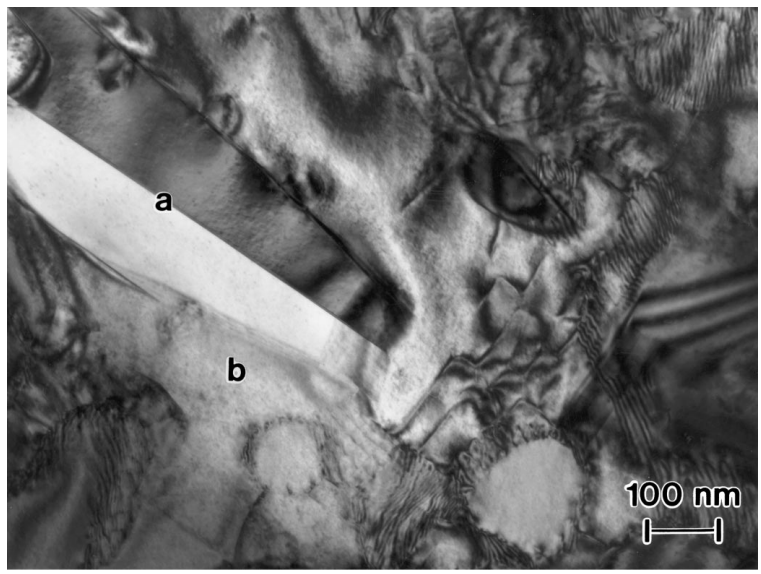

Figure 7 BF micrograph showing midrib twinned γ' (labeled as "a") with a surrounding precipitate free zone (indicated by "b") in a Ni-28 at % Al-18 at % Cr-6 at % Ti alloy aged for 140 h at 850 °C, producing a β/β' matrix.

relationship existed between the dendrite and interdendritic matrices).

The formation of γ' colonies (Fig. 8) constituted the third mode of γ' precipitation encountered in the present work. The typical size of precipitates within the colonies (generally about 200–500 nm long and up to around 100 nm wide) was roughly comparable with that of the individual midrib twinned γ' (generally about 250–700 nm long and up to around 250 nm wide) as discussed above. However, in the colonies, numerous precipitates were packed together with low angle boundaries separating the precipitates. Some, but not all, of these precipitates were twinned. When twinning was present, individual precipitates often contained multiple twins. As has already been discussed (see Section 3.1), titanium depletion from the dendrite matrix due to the formation of γ' layers and colonies had the effect of destabilizing the β'-phase.

Although γ' was the most important second-phase observed in the materials examined, other second phases were observed. In addition to the role of α-Cr in the formation of the β'-α eutectic, this phase was also a significant intradendritic second phase, especially after high temperature treatments. Typically, the intradendritic α precipitated (Fig. 9) in the form of spheroids with diameters of around 50–200 nm and semicoherent interfaces with the dendrite matrices. A cube–cube orientation relationship was observed between the intradendritic α and the β (or β') matrix.

After aging the Ni-26 at % Al-19 at % Cr-8 at % Ti alloy at 850 °C (Fig. 10), additional reflections were observed in $\mathbf{B} = [1\,1\,1]_{\beta'}$ diffraction patterns from the dendrite interiors. These reflections (Fig. 10a) consisted of faint additional spots located close to, but not exactly at, $\mathbf{g} = \frac{1}{4}\{1\,1\,0\}_{\beta'}$. Darkfield micrographs prepared from these additional reflections revealed that these

(a)

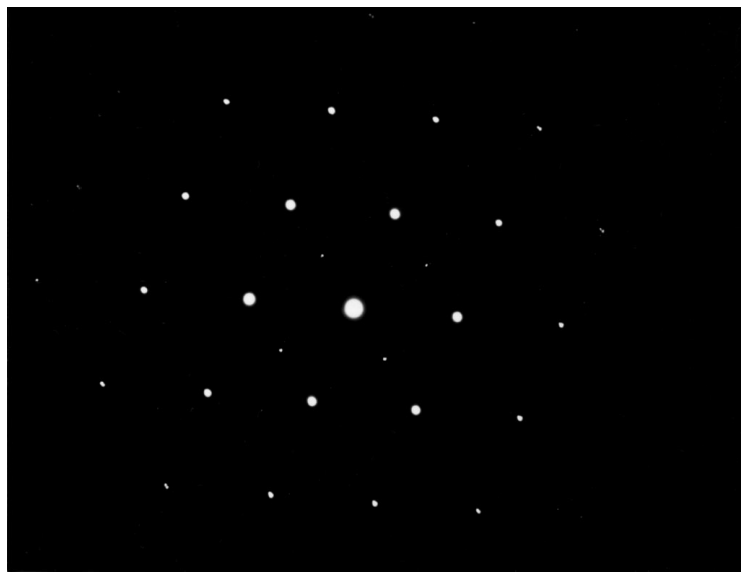

(b)

Figure 8 The formation of γ' colonies in the as-cast Ni-28 at % Al-18 at % Cr-6 at % Ti alloy: (a) DF micrograph with $\mathbf{g} = (1\,\bar{1}\,1)_{\gamma'}$, such that γ' appears bright and the surrounding β' matrix appears dark; (b) SAD pattern with $B = [1\,1\,0]_{\gamma'}$.

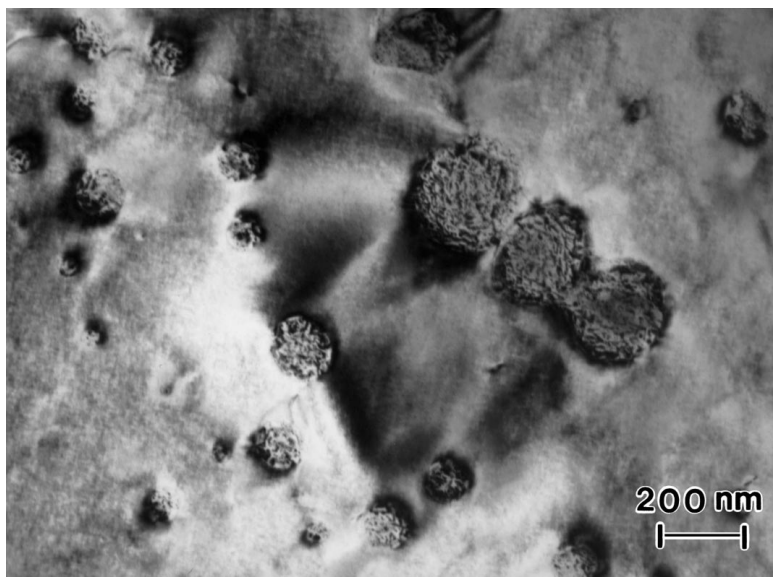

Figure 9 Intradendritic α-Cr precipitates in the as-cast Ni-28 at % Al-18 at % Cr-6 at % Ti alloy, imaged in BF.

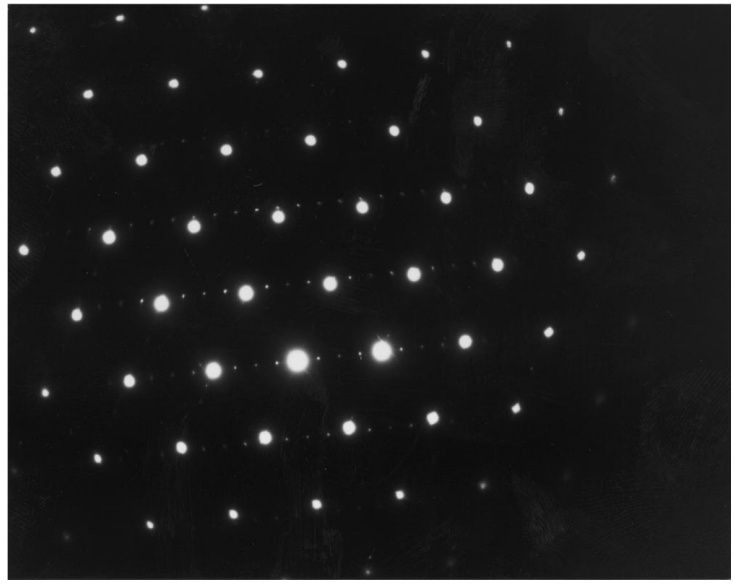

(a)

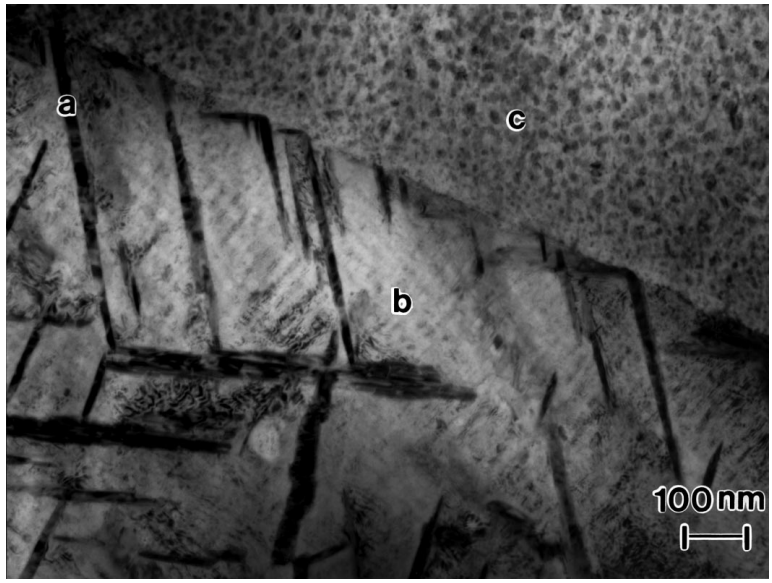

(b)

Figure 10 Needle-like features observed in the Ni-26 at % Al-19 at % Cr-8 at % Ti material aged for 140 h at 850 °C: (a) SAD pattern with $B = [1\,1\,1]_{\beta'}$ showing additional reflections; (b) BF micrographs showing needles (labeled as "a") precipitated on the interface between the dendrites (indicated by "b") and the interdendritic α-Cr (this is labeled as "c"—note the mottling of this region is due to the formation of fine β precipitates).

originated from elongated precipitates within the β' matrix. A given line of spots would all contribute to the same precipitate. These precipitates were observed to form within the bulk β', but also nucleated preferentially on the interfaces between the dendritic β'-phase and interdendritic α and then grew into the dendritic β' (Fig. 10b). Although the morphology of the precipitates resembled that of a portion of the γ' precipitates, there did not appear to be any direct connection between these two phases. Within the capabilities of TEM-based EDS analysis, the composition of the precipitates giving rise to the $\frac{1}{4}\{1\,1\,0\}_{\beta'}$ reflections appeared identical to that of the surrounding β'. One of the authors has previously [15] observed precipitates that produce additional reflections close to $\frac{1}{5}\{1\,1\,0\}_{\beta}$ positions, yet are similar in all other respects to the precipitates observed here. At the present time, it is uncertain if there is a connection between these two phases.

3.4. Mechanical properties

The room temperature tensile behavior of the Ni-28 at % Al-18 at % Cr-6 at % Ti alloy was evaluated in the as-cast condition, as well as after 850 and 1100 °C aging. This alloy contained a wide range of microstructural features and hence was selected for mechanical testing. These features differed significantly between the as-cast and the heat treated conditions. For instance, the as-cast microstructure of this alloy contained β' dendrite matrices and an eutectic between β' and α-Cr comprised the interdendritic regions. After the 850 °C aging treatment, partial transformation of β' resulted in a β'/β two phase mixture, both in the dendrite matrices and what was formerly the β' portion of the interdendritic eutectic. Further aging at 1100 °C fully transformed β', resulting in single-phase β dendrite matrices and a β-α-Cr interdendritic eutectic. It is to be noted that, in all the alloys examined, the dendrites occupied a

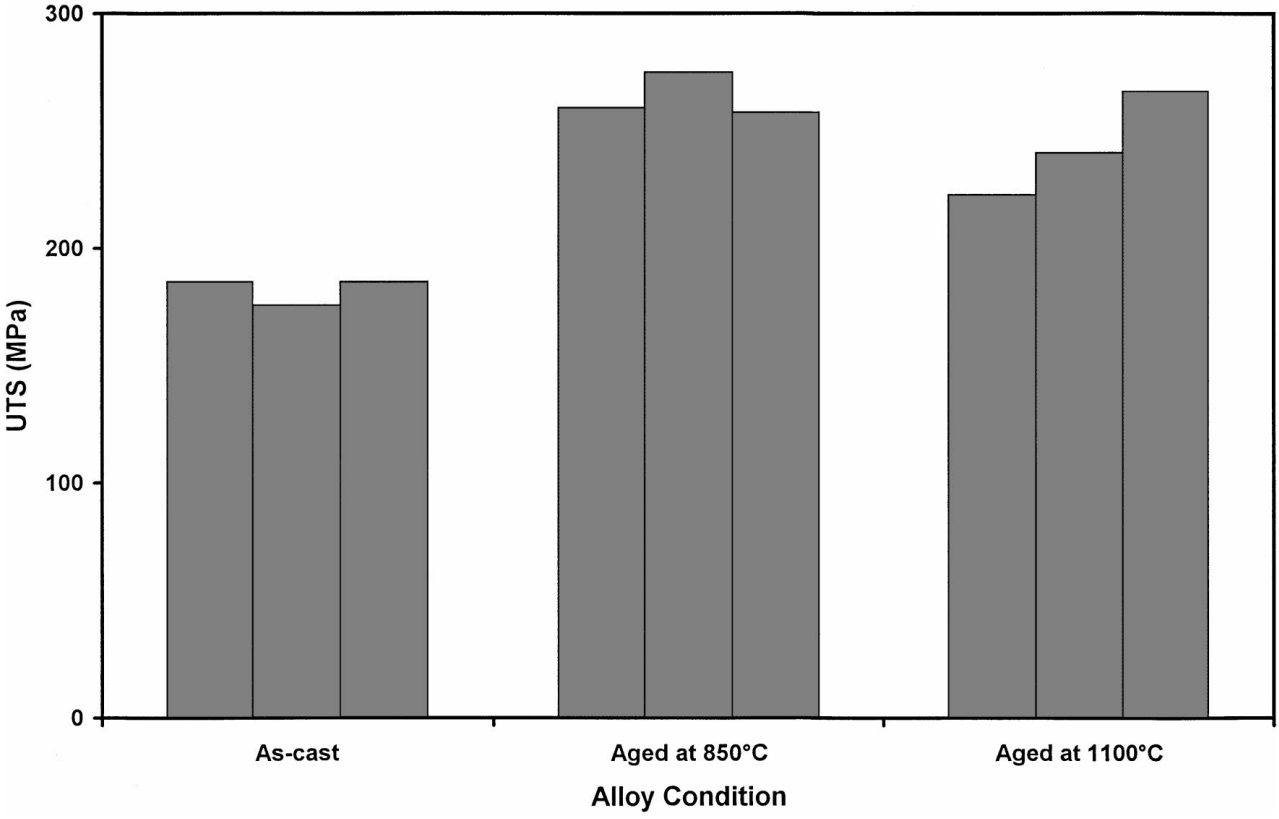

Figure 11 UTS data for the Ni-28 at % Al-18 at % Cr-6 at % Ti material in the as-cast conditions and after aging at 850 and 1100 °C for 140 h.

considerably larger volume fraction as compared to the interdendritic regions (Fig. 3). In the as-cast condition, a moderate number of α-Cr and γ' precipitates were present inter- and intradendritically. However, numerous new fine α-Cr precipitates were observed intradendritically after both heat treatments.

All of the materials tested showed brittle tensile behavior and no signs of plastic deformation were observed. The ultimate tensile strength (UTS) increased from an average of 186 MPa for the as-cast samples to mean values of 260 and 241 MPa for the 850 and 1100 °C heat treated samples, respectively (Fig. 11). The UTS values of the alloys with fully transformed β dendrite matrices (alloys aged at 1100 °C for 140 h) are in agreement with values determined by Weaver *et al.* for β-NiAl alloys [18].

SEM-based fractography (Fig. 12) showed invariably transdendritic fracture with the fracture path largely ignoring the interdendritic eutectics. Hence, the observed mechanical properties of the tensile samples

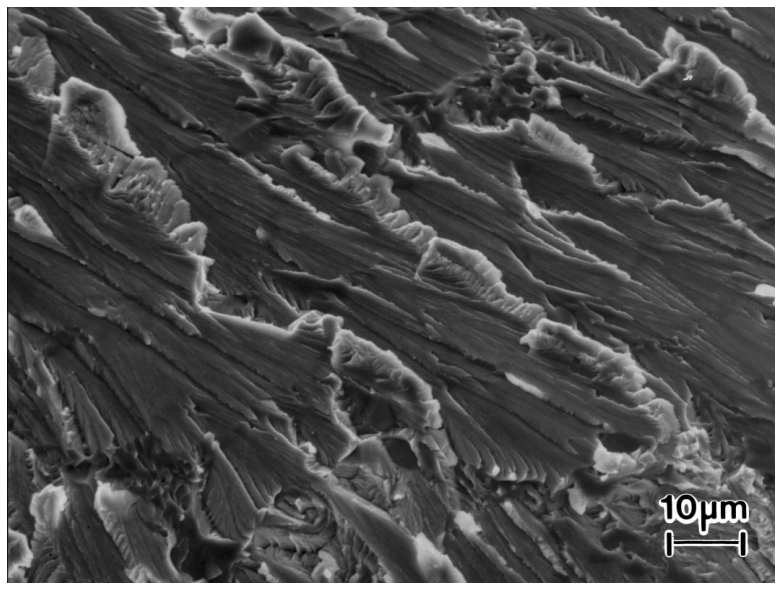

(a)

Figure 12 Fractographs (SEI) for the Ni-28 at % Al-18 at % Cr-6 at % Ti material: (a) As-cast; (b) Aged for 140 h at 850 °C; (c) Aged for 140 h at 1100 °C. (*Continued*).

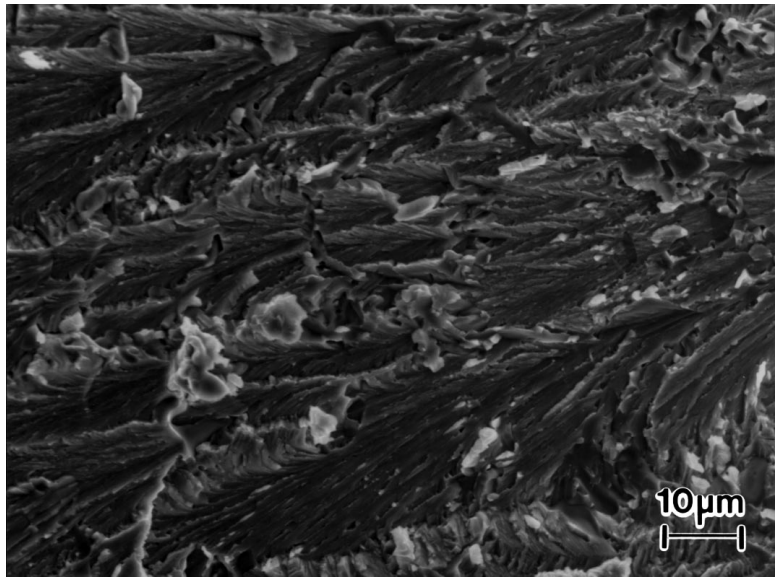

(b)

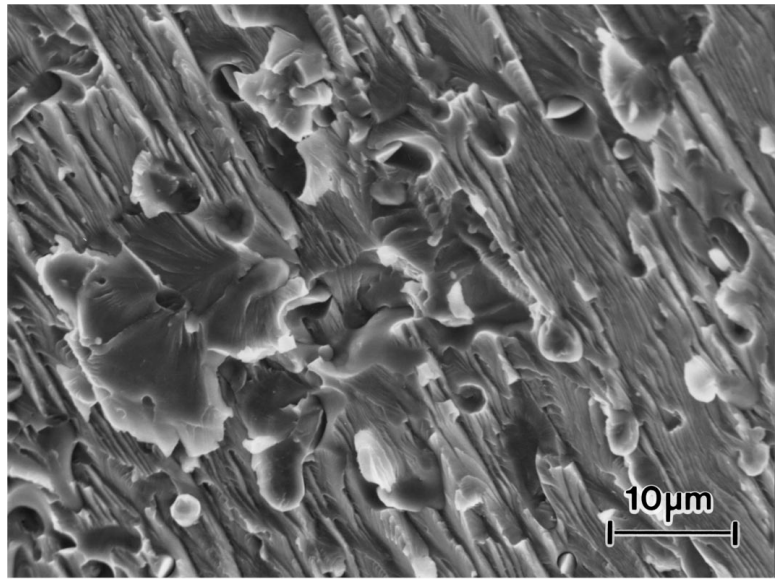

(c)

Figure 12 (*Continued*).

were essentially determined by the intradendritic microstructure of the tested alloys. Within the fractured dendrites, cleavage failure was noted in all cases, as shown in Fig. 12. The cleavage facets contained serrated surfaces, as previously observed by Tiwari *et al.* [19], on the fracture surface of binary β-NiAl.

In the present work, the fracture path of the single phase β' dendrite matrix alloy (as-cast) showed facets the typical size of which (around 30 μm) was essentially the same as that of the dendrites. In contrast, the size of the cleavage facets in the 850 °C aged fractured sample (in the range of 15–20 μm) was considerably smaller than that observed in the as-cast condition. The presence of a β'/β two phase mixture in this alloy might have caused the fracture path to constantly change direction on traveling from a β' to a β region. Furthermore, relatively tortuous fracture surfaces were noted for the heat treated alloys with numerous coarse (1 μm or larger) α-Cr precipitates. In contrast, the relatively flat fracture surface of as-cast condition samples showed facets with few, if any, α-Cr precipitates. Indeed, the pullout of these coarse α-Cr precipitates from the matrix was apparent (e.g. Fig. 12c). Presumably, the increase in UTS induced by aging resulted from a combination of the formation of numerous fine (100 nm or less) intradendritic precipitates of α-Cr as well as the presence of a β'/β two phase mixture.

The formation of a lamellar eutectic between α-Cr and β-NiAl has been previously shown to significantly enhance the room temperature fracture toughness of NiAl [20]. However, in the present samples, the interdendritic regions were relatively small and isolated, rather than forming a continuous layer around the dendrites. In these samples, the fracture path did not pass through the interdendritic regions.

4. Conclusions

An investigation of the microstructure and mechanical properties of three cast alloys derived from the B2 type β-NiAl phase and containing 26–30 at % Al 18–21 at % Cr and 4–8 at % Ti was conducted. As a result of

this investigation, the following conclusions have been drawn:

- All of the materials investigated solidified dendritically to β'. In all cases, solidification terminated with the formation of a β'-α lamellar eutectic.
- With the exception of the high titanium (8 at %) alloy, thermal exposure at 850 °C tended to destabilize the dendritic and interdendritic β' to different degrees. Full transformation of β' to β was associated with low titanium levels (4 at %). While partial transformation in the moderate titanium content alloys (6 at %) resulted in a β'/β two phase mixture. However, in most cases, the stability of the resulting two phase β'/β was limited with respect to the 1100 °C treatment.
- Two modes of β' transformation were observed. The first of these involved depletion of titanium from the matrix by the formation of titanium-bearing γ' during aging. Even in the as-cast condition, the formation of γ' colonies scavenged titanium from the β' phase, resulting in β dendrite matrices in the vicinity of these colonies. The second mode of β' transformation occurred with no change in the titanium content of the transformed region and was not associated with the precipitation of γ' from the matrix.
- Microstructural development in the materials investigated was substantially complicated by a range of different modes of γ' and α-Cr precipitation. In the case of γ', precipitation occurred both as individual second-phases within the β' (or β) phase and as a variety of colonies of more-or-less single phase γ'. In addition to the role of the α-phase in the eutectic, α also constituted a significant intradendritic second-phase.
- All the materials investigated showed a brittle tensile behavior. The fracture path cleaved through the dendrites of all alloys. Due to the small volume fraction occupied by the interdendritic eutectics, the mechanical properties were largely determined by the microstructure of the dendritic regions.
- The presence of β'/β two phase mixture and numerous second phase precipitates (α-Cr and γ'), due to thermal exposures of 140 h at 850 °C, correlated with the increase in UTS values of the alloys from around 186 MPa in the as-cast condition to 260 MPa. Conversely, heat treatments at 1100 °C resulted in single-phase β matrix alloys with mean UTS values of 241 MPa.

Acknowledgements

The research described in this paper was supported by the National Science Foundation's EPSCoR Program.

References

1. D. B. MIRACLE, *Acta Metall. Mater.* **41** (1993) 649–684.
2. P. S. KHADKIKAR, K. VEDULA and B. S. SHABEL, *MRS Symp. Proc.* **81** (1987) 157–164.
3. S. GUHA, P. R. MUNROE and I. BAKER, *ibid.* **133** (1989) 633–638.
4. K. ISHIDA, R. KAINUMA, N. UENO and T. NISHIZAWA, *Metall. Trans. A* **22A** (1991) 441–446.
5. R. D. FIELD, D. D. KRUEGER and S. C. HUANG, *MRS Symp. Proc.* **133** (1989) 567–572.
6. M. LARSEN, A. MISRA, S. HARTFIELD-WUNSCH, R. D. NOEBE and R. GIBALA, *ibid.* **194** (1990) 191–198.
7. A. MISRA, R. D. NOEBE and R. GIBALA, *ibid.* **273** (1992) 205–210.
8. *Idem., ibid.* **288** (1993) 483–488.
9. P. R. STRUTT and B. H. KEAR, *ibid.* **39** (1984) 279–292.
10. R. YANG, J. A. LEAKE and R. W. CAHN, *J. Mater. Res.* **6** (1991) 343–354.
11. I. E. LOCCI, R. M. DICKERSON, A. GARG, R. D. NOEBE, J. D. WHITTENBERGER, M. V. NATHAL and R. DAROLIA, *ibid.* **11** (1996) 3024–3038.
12. W. F. GALE and J. E. KING, *Mater. Sci. Technol.* **9** (1993) 793–798.
13. *Idem., J. Mater. Sci.* **28** (1993) 4347–4354.
14. *Idem., Metall. Trans. A* **23A** (1992) 2657–2665.
15. W. F. GALE, T. C. TOTEMEIER and J. E. KING, *Metall. Mater. Trans. A* **26A(4)** (1995) 949–956.
16. *Idem., Microst. Sci.* **21** (1994) 61–80.
17. W. F. GALE and Z. A. M. ABDO, *J. Mater. Sci.* **33** (1998) 2299–2304.
18. M. L. WEAVER, R. D. NOEBE, J. J. LEWANDOWSKI, B. F. OLIVER and M. J. KAUFMAN, *Mater. Sci. Engin.* **A192/193** (1995) 179–185.
19. R. TIWARI, S. N. TEWARI, R. ASTHANA and A. GARG, *ibid.* **A192/193** (1995) 356–363.
20. F. E HEREDIA, M. Y. HE, G. E. LUCAS, A. G. EVANS, H. E. DEVE and D. KONITZER, *Acta. Metall. Mater.* **41** (1993) 505–511.

Received 30 September 1998
and accepted 11 February 1999